

Nanoscale phase separation in $\text{La}_{0.7}\text{Ca}_{0.3}\text{MnO}_3$ films: evidence for the texture driven optical anisotropy

A.S. Moskvina and E.V. Zenkov
Ural State University, 620083 Ekaterinburg, Russia

Yu.P. Sukhorukov, E.V. Mostovshchikova, and N.N. Loshkareva
Institute of Metal Physics, Ural Division of Russian Academy of Sciences, 620219 Ekaterinburg, Russia

A.R. Kaul and O.Yu. Gorbenko
Moscow State University, 119899 Moscow, Russia

The IR optical absorption ($0.1 \text{ eV} < \hbar\omega < 1.5 \text{ eV}$) in the $\text{La}_{0.7}\text{Ca}_{0.3}\text{MnO}_3$ films on LaAlO_3 substrate exhibits the drastic temperature evolution of the spectral weight evidencing the insulator to metal transition. Single crystal films were found to reveal strong linear dichroism with anomalous spectral oscillations and fairly weak temperature dependence. Starting from the concept of phase separation, we develop the effective medium model to account for these effects. The optical anisotropy of the films is attributed to the texturization of the ellipsoidal inclusions of the quasimetal phase caused by a mismatch of the film and substrate and the twin texture of the latter.

PACS numbers: 71.27, 64.75, 75.50.T, 78.67.B

Keywords: manganites, phase separation, effective medium, linear dichroism

I. INTRODUCTION

The investigation of doped rare-earth manganites has a long history, starting from 1950th. The intense researches of last decade, stimulated with the discovery of colossal magnetoresistance have enriched significantly our understanding of these systems. However, recent studies argue its internal nature to be by far more complex as compared to what is predicted by the conventional phase diagrams^{1,2}. In particular, there is a growing experimental evidence^{3,4,5} in favour of a generic nanoscale inhomogeneity of manganites as well as many other strongly correlated transitional metal oxides^{6,7}.

The infrared (IR) optical studies⁸ of $\text{La}_{1-x}\text{Ca}_x\text{MnO}_3$ ($0.1 < x < 0.8$) were one of the first to attest the phase separation in manganites. The analysis of diffuse neutron scattering studies of spin correlations in $\text{La}_{1-x}\text{Ca}_x\text{MnO}_3$ ($x < 0.2$) single crystals⁹ confirms the existence of ferromagnetic (FM) inhomogeneities below T_c in the form of platelets with a mean diameter of about 16 Å.

In the films, unlike as in the bulk samples, the phase-separated state can persist at still higher doping probably due to the specific properties of the film-substrate interface stabilizing the novel phase. Indeed, the atomic force microscopy of $\text{La}_{0.67}\text{Ca}_{0.33}\text{MnO}_3$ films deposited on LaAlO_3 substrate⁵ yields a direct visualization of coexisting FM metallic and charge-ordered insulating phases. The authors suggest the key factor governing the occurrence of this phase separation to be the mismatch of the film and the substrate, resulting in nonuniform compressive strains of the lattice and concomitant inhomogeneities in exchange and hopping parameters. The low strain well conducting islands with mean size as large as 500 Å, separated by high strain insulating interfaces are clearly discernible on the micrographs of the film.

In this paper we present the results of optical studies of strained $\text{La}_{0.7}\text{Ca}_{0.3}\text{MnO}_3$ films, that can be considered as another possible manifestation of intrinsic phase inhomogeneity of these systems. Surprisingly enough, the IR absorption spectra display significant optical anisotropy and unusual oscillating frequency dependence of the dichroism, that cannot be associated with a certain electronic transitions. Our model calculations, based on the concept of strain-induced ordering of prolate quasimetal droplets in parent insulator, agree quantitatively with experiment.

II. EXPERIMENTAL

Two $\text{La}_{0.7}\text{Ca}_{0.3}\text{MnO}_3$ (LCMO) manganite films, 60 nm and 300 nm in thickness, were grown on single crystalline (001) oriented LaAlO_3 (LAO) substrates. The details of films growth and sample characterization are given elsewhere^{10,11}. The X-rays diffraction patterns and high resolution transmission electron microscopy confirm the epitaxial character of the films. The rocking curve method yields $\text{FWHM} = 0.16^\circ$, that implies small mosaicity and high quality orthorhombic $Pnma$ structure of the films. The out-of-plane lattice constants c 's (3.870 Å (60 nm) and 3.872 Å (300 nm)) are close to the in-plane ones (3.863 Å (60 nm) and 3.862 Å (300 nm)) for both films, so that structural anisotropy is small. We note a small amount of Mn_2O_3 impurity in the thick (300 nm) film, that does not alter the perovskite structure of the sample and is observed in the form of nanoscale inclusions in epitaxial matrix.

The optical experiments were performed in the range of $0.1 < \hbar\omega < 1.5 \text{ eV}$, $80 < T < 295 \text{ K}$ using automatic prismatic spectrometer. The absorption coefficient (K)

was derived from the measured ratio of transmitted to incident beam intensities as $K = (1-d) \ln(1-R)^2 I_0 = I$, d and R being the film thickness and the reflectance, respectively. The grating polarizer was employed in IR region. The spectra were taken for the light wave E -vector, adjusted along and normally to the direction of maximal absorption (c -axis), determined by the rotation of the polarizer. As usual, the linear dichroism is defined as

$$= \frac{K(E \parallel c) - K(E \perp c)}{K(E \parallel c) + K(E \perp c)}; \quad (1)$$

where K 's are the absorption coefficients for appropriate polarizations.

III. RESULTS AND DISCUSSION

A. Optical spectra

The IR optical response of doped manganites such as $\text{La}_{1-x}(\text{Sr};\text{Ca})_x\text{MnO}_3$ differs strongly from those of pure LaMnO_3 system. A self-consistent description of the charge-transfer (CT) bands in LaMnO_3 ¹² shows the multiband structure of the CT optical response with the weak low-energy edge at 1.7 eV, associated with forbidden $t_{1g}(\pi) \rightarrow e_g$ transition. These predictions are in a good agreement with experimental spectra. A common feature of doped manganites and related systems is revealed in an unconventional enhancement of IR spectral weight, evidencing the appearance of free charge carriers contribution.

The absorption spectra of thin (60 nm) film are shown in Fig.1A. At $T = 295$ K the unpolarized light IR spectrum displays an insulating gap-like behavior. However, this behaviour is unusual, since the absorption, without being metallic, remains rather large in entire spectral range. The increase of absorption coefficient below a dip near 0.2 eV is related to phonon bands, starting at 0.09 eV,

The lowering of temperature to 80 K, well below the Curie temperature $T_c = 268$ K, entails a drastic enhancement of IR spectral weight, straightforwardly evidencing the appearance of free charge carriers contribution. Very large free carriers absorption of thick (300 nm) film at $T = 80$ K makes the transmission experiments difficult, so that in FM region the measurements were performed only around T_c (Fig.1C). We observed quite similar behaviour also in self-doped $\text{La}_{0.83}\text{MnO}_3$ ¹³ and $\text{La}_{0.7}\text{Sr}_{0.3}\text{MnO}_3$ film¹⁴. Comparative analysis of these spectra with those of other doped manganites ($\text{La}_{1-x}(\text{Sr};\text{Ca})_x\text{MnO}_3$ ^{15,16}, $\text{Nd}_{1-x}\text{Sr}_x\text{MnO}_3$ ¹⁷, etc.) allows us to conclude, that here we deal with the seemingly universal physical behavior, common to a wide family of doped manganites. Earlier, we assigned^{13,18,19} this unconventional optical response to nanoscopically inhomogeneous texture of manganites which looks like a system of metallic droplets in insulating matrix. The spec-

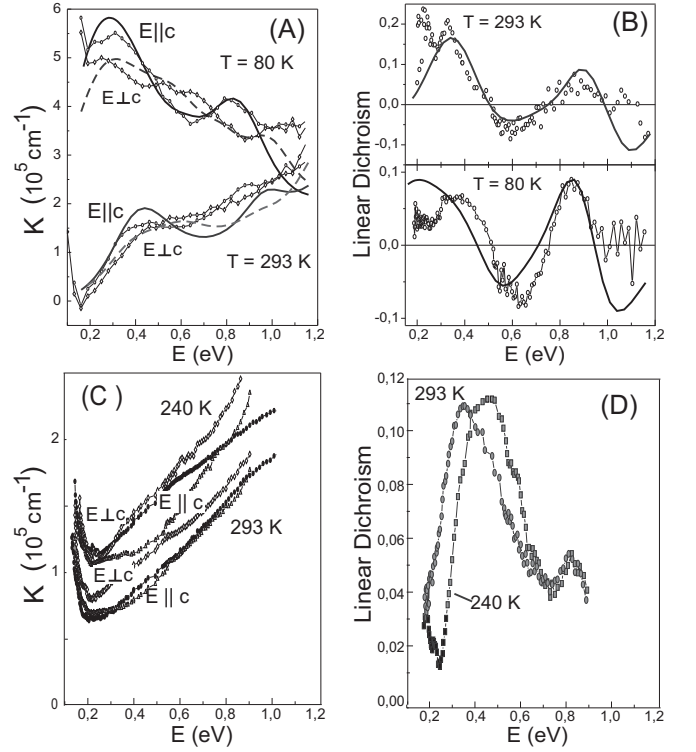


FIG. 1: Top panel: Spectroscopic data for thin (60 nm) $\text{La}_{0.7}\text{Ca}_{0.3}\text{MnO}_3$ film at $T = 80$ K and $T = 293$ K. (A) Absorption spectra for two polarizations: experimental data are shown by dots, curves are the result of fitting in frames of effective medium theory (the unpolarized light spectra are not shown). (B) Linear dichroism spectra: experiment (dots) and effective medium theory (curves).

Bottom panel: Spectroscopic data for thick (300 nm) $\text{La}_{0.7}\text{Ca}_{0.3}\text{MnO}_3$ film at $T = 240$ K and $T = 293$ K. (C) Absorption spectra: unpolarized light (circles), $E \parallel c$ polarization (triangles), $E \perp c$ polarization (diamonds). (D) Linear dichroism spectra.

tral features are believed to be governed mainly by the temperature dependent metallic volume fraction and geometrical resonances in a nanoscopically inhomogeneous system. From theoretical standpoint, the possibility of the phase separation in manganites has been examined in pioneering work by Nagaev²⁰, developed afterwards²¹. It was shown, that the competition of hopping energy and double exchange render the charge carriers segregation in nanoscopic FM conducting droplets (ferrons) energetically favorable as compared to uniform spin-canted state. Such a segregation is accompanied with the gradual shift of the spectral weight from the absorption bands of parent AF matrix to lower-energy excitations in the droplets of a novel phase.

The experiments in polarized light revealed the interesting features, observed in IR absorption spectra of thin film both in FM and paramagnetic (PM) states, viz. the oscillations about the unpolarized light spectrum (Fig.1A). The spectra of thick films look differently (Fig.1C). Above T_c , the absorption coefficient in $E \perp c$

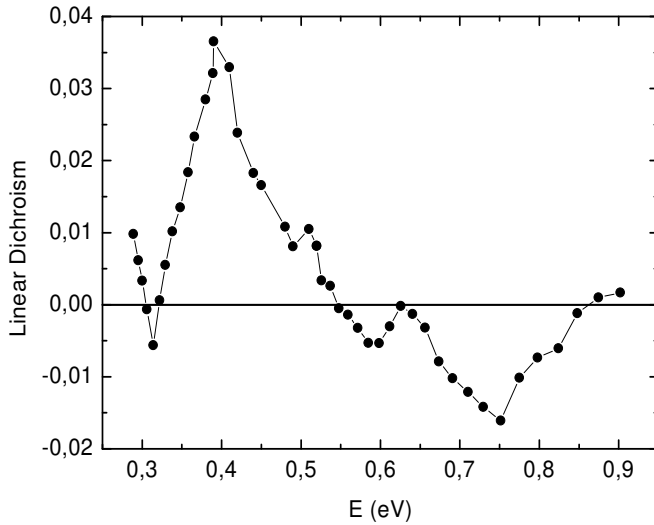


FIG. 2: The linear dichroism of the LAO substrate.

c polarization exceeds in magnitude that in unpolarized light, while in E k c polarization these spectra nearly coincide over the range 0.2 to 0.9 eV. In FM state (240 K), the E ? c and unpolarized spectra are indistinguishable in 0.2–0.5 eV range, but above 0.5 eV the absorption coefficient in the E ? c polarization shows more rapid increase. The E k c spectrum approaches the unpolarized one from below and intersects at 0.8 eV.

The above peculiarities of polarized light absorption manifest itself in the spectral oscillations of the linear dichroism of thin film with the amplitude of the order of 0.3 about zero (Fig.1B). The dichroism in thick film is positive throughout the spectral range 0.2–0.9 eV with two peaks, at 0.4 eV and 0.8 eV, which position is close to that observed in the dichroism spectrum for thin

film (Fig.1D). It should be noted, that upon cooling from $T = 293$ K to $T = 240$ K, the low-energy peak blue-shifts from 0.35 to 0.45 eV.

B. Discussion

Nontrivial questions arise about the origin of the observed peculiarities of optical response, since no allowed electro-dipole transitions are known to fall in the spectral range under consideration. It is worthy of noting that the LAO substrate reveals itself the optical anisotropy, most probably due to a twinning. However, its absorption in the spectral range under examination is negligibly small as compared with that observed for LCMO/LAO films. Hence, small dichroism of substrate with its irregular spectral dependence (see Fig. 2) can be neglected in our further discussion.

While the magnitude of the absorption coefficient for the films varies by hundreds of percents upon cooling from $T = 293$ K to $T = 80$ K, the behaviour of dichroism remains practically unchanged both in PM and FM states, and its amplitude does not change significantly

when turning from the thin film to the thick one. Note, that the dichroism is observed in both films and thus is not related to the Mn_3O_4 impurity effects. However, restricting ourselves to the conventional explanations, we may overlook another possibilities, stemmed from the intrinsic nanoscale phase inhomogeneity of doped manganites. In particular, we assume, that under the mismatch induced nonuniform stresses, the droplets of the quasimetallic phase may align to form somewhat like a nematic liquid crystal. Such a texture, reflecting the twin pattern of the substrate, results in a significant enhancement of the observed dichroism of the LCMO=LAO

films. We show, that this model, being the development of our general approach to manganites as nanoscopically inhomogeneous systems^{13,18,19}, can provide a good quantitative agreement with all experimental findings presented in the previous section.

First, we would like to shortly overview the effective medium theory (EMT)²² which appears to be a powerful tool for the quantitative description of the optical response of inhomogeneous systems. In its simplest form, the EMT equation for effective dielectric function ϵ_{eff} of the two-component inhomogeneous system reads as follows²²:

$$\int_V dV p(\mathbf{r}) \sum_{i=1}^2 \frac{\epsilon_i^3}{\epsilon_{eff} + L_i (\epsilon_i - \epsilon_{eff})} = 0; \quad (2)$$

where the integration runs over the volume of the sample, $p(\mathbf{r}) = p_1(\mathbf{r})\epsilon_1 + p_2(\mathbf{r})\epsilon_2$. We consider the two components of binary composite on equal footing with $p_{1,2}$ being the volume fractions, $\epsilon_{1,2}$ and L_i the dielectric functions and the depolarization factors of the grains of its constituents, respectively.

It is worth to emphasize that in effective medium approximation the volume of the droplet does not enter the calculations, but is accounted implicitly in the validity range of the theory, restricting the mean size of the droplet to be smaller than the wavelength. Hence, within the EMT, the volume fractions $p_{1,2}$ can only change through the number of the droplets rather than due to the variation of their sizes. In general, $p_{1,2}$ are determined by thermodynamical conditions and depend on temperature, pressure, and other external factors. The approach²³, we employed here to lend more plausibility to this physically transparent EMT scheme, is to take into account the natural difference between the core and the surface properties of the inclusions using the standard expression for the polarizability of the coated ellipsoid²⁴.

The spectra of nanoscopically disordered media display some specific features due to geometric resonances²², that have no counterpart in homogeneous systems. These arise as a result of resonant behaviour of local field corrections to the polarizability of the granular composite and are governed to a considerable extent by the shape of the grains. The frequency of geometric resonance is then easily obtained as the one at which the polarizability of small particle diverges. For the case of spherical

metallic droplets embedded in the insulating matrix with dielectric permittivity ϵ_d this leads to the equation:

$$\epsilon(\omega)_{\text{part}} + 2\epsilon_d = 0; \quad (3)$$

whence the resonance frequency is

$$\omega_r = \omega_p \frac{1}{1 + 2\epsilon_d}; \quad (4)$$

if the Drude's expression with the plasma frequency ω_p is assumed for the metallic permittivity and ϵ_d is constant. In the case of arbitrary ellipsoid there are three different principal values of polarizability and the latter formula generalizes to

$$\epsilon_r^i = \omega_p^2 \frac{L_i}{\epsilon_d (L_i (\epsilon_d - 1))}; \quad i = 1; 2; 3; \quad (5)$$

where L_i are three shape-dependent depolarization factors. For the cubic matrix it is naturally to assume these ellipsoidal droplets to be oriented along main symmetry directions like $[111]$, $[100]$.

Such a simple model of phase separation enables us to understand the nature of linear dichroism observed in LCMO=LAO films both above and below T_c even without any assumptions concerning the intrinsic electronic anisotropy of its constituents. Indeed, for a bulk magnetite crystal with cubic symmetry all orientations of ellipsoidal droplets like $[111]$ are energetically equivalent and equally distributed that restores the high symmetry of the system as a whole and results in the optical isotropy of nanoscopically phase-separated sample. However, any anisotropic noncubic perturbation like strain lifts the orientational degeneracy of ellipsoidal droplets and gives rise to a certain texture. When this texture is irradiated by a plane wave, the geometric resonances (Eq. 5) will be excited selectively depending on the polarization. Thus, the phase-separated sample as a whole can exhibit sizable optical anisotropy in the spectral range of the geometric resonances. Namely such a situation is likely to occur in our samples due to the unavoidable mismatch of the film and the substrate that generally results in non-uniform strains, that can favor some ordering of the droplets to form a texture. Since the film and the substrate have the same lattice structure, their mismatch would in principle result in bulk contraction, changing the volume of the unit cell. The magnetite films grown on LAO substrate are known²⁵ to be under compressive stress, their lattice being contracted in the plane and expanded in the normal direction. High energy cost of this deformation makes more feasible the relaxation channel that implies the nonuniform distribution of the metal volume fraction with the density enhanced near the LCMO=LAO interface. Indeed, the lesser volume of the unit cell for metallic phase as compared with insulating LCMO matrix provides the optimal relaxation of the mismatch. However, the large density of metallic ellipsoidal droplets implies its ordering, or packing along one of four equivalent directions in the plane of film. In our case this direction

is likely to be determined by the twin texture observed for LAO substrate. In such a way we come to the nucleation of the three-dimensional texture of metallic ellipsoidal droplets resulting in the optical anisotropy of the film. Our preliminary experimental examinations of the optical anisotropy of the twinned single-crystalline $\text{La}_{0.93}\text{Ce}_{0.07}\text{MnO}_3$ sample also argue in favour of this picture. Note, that in all cases the resulting deformation of the lattice may be quite small to be detected by conventional X-ray methods.

To check the validity of the hypothesis of the texture-driven dichroism in LCMO=LAO films we simply assumed the nanoparticles to be identically aligned along the optical axis in the plane of the film, so that the amplitude of the dichroism would be governed only by their shape anisotropy. To this end, leaving only one of the terms in the sum (Eq. 2), we are in the position to calculate the eigenvalues of effective dielectric tensor and to simulate the dichroism. For the model to be more realistic we assume the metallic-like droplet in the form of coated ellipsoid which dielectric function can be written as follows²⁴:

$$\epsilon_i = \epsilon_{\text{out}} \frac{(\epsilon_{\text{in}} - \epsilon_{\text{out}}) (f L_i^{\text{out}} L_i^{\text{in}} f) \epsilon_{\text{out}}}{(\epsilon_{\text{in}} - \epsilon_{\text{out}}) (f L_i^{\text{out}} L_i^{\text{in}}) \epsilon_{\text{out}}}; \quad (6)$$

where L 's are the depolarization factors of inner (in) and outer (out) confocal shells (core and coating, respectively), f is the core to coating volume ratio for this composite inclusion. Leaving aside the question of the microscopic electronic structure of the droplet, we described its core and the coating by the Drude formula:

$$\epsilon = \epsilon_0 \frac{\omega_p^2}{\omega(\omega + i\gamma)} \quad (7)$$

where ω_p is the plasma frequency, γ is the damping parameter. This approximation is reasonable and is more general that it may seem, since the Drude form can be regarded as a limiting form of the universal expression for dynamical conductivity in terms of memory function²⁶ with ω_p and γ to be effective parameters. Imaginary part of dielectric function of LaMnO_3 was fitted to experiment¹⁵ by the sum of three gaussian in a broad spectral range to ensure the validity of its real part, derived via Kramers-Kronig transformation. Note, that the phonon bands have been neglected throughout the calculations. The energies, intensities and damping constants (ω and γ being in units of eV) of gaussians are: $(\omega; I; \gamma) = (2.5; 2.6; 0.777); (5.0; 7.8; 0.929); (6.5; 2.866; 0.697)$.

The main results of our calculations are shown in the Figs. 1 A, B. The room temperature spectra were fitted given the following parameters: the volume fraction of quasi-metal phase $p = 0.1$, $f = 0.4$, $\omega_{p1} = 3.0$ eV, $\omega_{p2} = 1.35$ eV, $\gamma_1 = 0.3$ eV, $\gamma_2 = 0.4$ eV, where the indices 1;2 stand for the core and the coating of the quasi-metal droplet, respectively. The ratio of in-plane semiaxes of quasi-metal inclusions is set equal to

$b/a = 0.5$ and out-of-plane to major in-plane equal to $c/a = 0.42$. In principle, the quantum size effect in a small nonspherical particle would bring about an anisotropic contribution to the relaxation rate. For the sake of simplicity, we neglected this small effect in our model calculations.

As follows from the experiment, the lowering of the temperature shifts the phase equilibrium toward the "metalization", drastically expanding the volume fraction of the metallic droplets. However, while the system becomes more metallic, it may not be necessarily the case for an individual droplet because of the noise, the random overlaps with neighbour droplets introduce in its surrounding, so that the volume of the core relative to the fluctuating edge region may even get smaller. To simulate the low-temperature spectra, we modified the parameters (ϵ and κ kept fixed) as follows: $p = 0.55$, $f = 0.23$, $\hbar\omega_{p1} = 2.4$ eV, $\hbar\omega_{p2} = 1.12$ eV, $\hbar\omega_1 = 0.3$ eV, $\hbar\omega_2 = 0.3$ eV. Thus, for a fixed doping, the temperature appears to be a main physical parameter, governing the metallic volume fraction and percolation. The intrinsic "electronic" parameters like $\hbar\omega_p$ and κ , roughly speaking, are temperature independent with the accuracy of the order of 10–20%. The both results point toward the sound structure of our simple model. Although it can hardly provide the excellent fit of experiment throughout entire spectral range, it still captures the essential features of the dichroism spectrum despite of a great body of obvious simplifying assumptions. The two-peaked structure of the absorption coefficients, that combines according to Eq. (1) to provide the oscillations of the dichroism, results from the superposition of geometric (Mie's) resonances, governed by a fine tuning of the parameters. It should be noted that the model can yield rather complex behaviour of the spectra with multiple resonances. At the same time it is worth noting, that similar calculations with simple ellipsoidal particles fail to reproduce all the peculiarities of the absorption and dichroism spectra. This means, that one should take care of the internal structure of the nanoparticles when employing the EM T in realistic models.

In conclusion, we reported the IR transmission measurements of the LCMO MnS grown on LAO substrate. Upon cooling from the room temperature to $T = 80$ K, the absorption coefficient of thin MnS was found to rise markedly. The main finding of the present studies is unconventionally large nearly temperature independent lin-

ear dichroism of the MnS , and its spectral oscillations, unexpected in view of the good structural perfection of the samples. We assert these features to be the manifestation of the inhomogeneous phase-separated state of the MnS . The optical anisotropy of the MnS is attributed to the texturization of the ellipsoidal nanoparticles of the quasimetal phase caused by a mismatch of the MnS and substrate and the twin texture of the latter. The simulation in frames of an effective medium model provided a good description of experiment. Despite this, at present we cannot exclude another possible scenarios of linear dichroism in manganite MnS , in particular, the magnetic one. Indeed, our model implies the intrinsic ferromagnetic ordering of quasimetallic droplets with superparamagnetic behavior at $T > T_C$ and magnetic percolation below T_C . Such a ferromagnetic droplet would manifest a magnetic linear dichroism irrespective of its shape. However, for the MnS to reveal the linear dichroism we need its relevant magnetic texture, or some kind of the ordering of the droplets. One should note that similar to our model the quantitative description of magnetic mechanism may be carried out in frames of effective medium theory. Actually, the distinction of two mechanisms needs in further studies.

In any case we see, that the analysis of the optical anisotropy provides the effective tool for the examination of nanoscale texture of the MnS . More generally, we suggest that the results of present paper as well as a great body of previous contributions^{5,6,9,13} have to enrich and extend the conventional understanding of the optical response of manganites, demonstrating the importance of specific effects of its intrinsic nanoscale phase inhomogeneity. In particular, we may state that the specific properties of dichroism in the spectral range 0.1 eV $< \hbar\omega < 1.5$ eV support our model^{13,18,19} in which the appropriate optical response is governed mainly by the geometrical resonances in nanoscale inhomogeneous system.

Acknowledgments

The work was supported by INTAS 01-0654, Federal Program (Contract No. 40.012.1.1. 1153-14/02), grants RFBR No. 01-02-96404, No. 02-02-16429, RFMC No. E00-3.4-280, CRDF No. REC-005 and UR 01.01.042.

Electronic address: eugene.zenkov@usu.ru

¹ A. Urushibara, Y. Morimoto, T. Arima et al., Phys. Rev. B 51, 14103 (1995)

² P. Schier, A. P. Ramirez, W. Bao, and S.-W. Cheong, Phys. Rev. Lett. 75, 3336 (1995)

³ E. L. Nagaev, Usp. Fiz. Nauk 166, 833 (1996) [Phys.-Uspekhi 39, 781, (1996)]

⁴ M. B. Salamon, M. Jain, Rev. Mod. Phys. 73, 583 (2001)

⁵ A. Biswas, M. Rajeswari, R. C. Srivastava et al., Phys. Rev. B 61, 9665 (2000); Phys. Rev. B 63, 184421 (2001)

⁶ S. H. Pan, J. P. O'Neal, R. L. Badzey et al., Nature, 413, 282 (2001)

⁷ M. Uehara, S. Mori, C. H. Chn, S.-W. Cheong, Nature (London), 399, 560 (1999)

⁸ N. N. Loshkareva, Yu. P. Sukhonukov, S. V. Naumov et al. JETP Lett. 68, No. 1, 97 (1999).

- ⁹ G. Biotteau, M. Hennion, F. Mousa et al., Phys. Rev. B 64, 104421-1 (2001)
- ¹⁰ O. Yu. Gorbenko, A. R. Kaul, N. A. Babushkina, L. M. Belova, J. Mater. Chem. 7, 747 (1997)
- ¹¹ O. Yu. Gorbenko, I. E. Graboy, A. R. Kaul, H. W. Zandbergen, J. Mater. Phys. 211, 97 (2000)
- ¹² A. S. Moskvina, Phys. Rev. B 65, 205113 (2002); cond-mat/0111198
- ¹³ Yu. P. Sukhorukov, N. N. Loshkareva, E. V. Mostovshchikova, A. S. Moskvina, E. V. Zenkov et al., JETP (to be published)
- ¹⁴ N. N. Loshkareva, Yu. P. Sukhorukov, V. E. Arhipov et al., Solid State Physics, 41, 426 (1999).
- ¹⁵ K. Takenaka, K. Iida, Y. Sawaki et al. J. Phys. Soc. Japan, 68, 1828 (1999)
- ¹⁶ J. H. Jung, K. H. Kim, D. J. Eom et al. Phys. Rev. B 55, 15489 (1997)
- ¹⁷ H. J. Lee, J. H. Jung, J. S. Lee et al., Phys. Rev. B 60, 5251 (1999)
- ¹⁸ A. S. Moskvina, E. V. Zenkov, Yu. D. Panov, Solid State Physics, 44, 1519 (2002).
- ¹⁹ Yu. P. Sukhorukov, N. N. Loshkareva, E. A. Gan'shina et al. JETP 92, No. 3, 462 (2001).
- ²⁰ E. L. Nagaev, Pis'ma v JETPh 16, 558 (1972)
- ²¹ D. I. Khomskii, Physica B 280, 325 (2000); M. Yu. Kagan, D. I. Khomskii, M. V. Mostovoy, Eur. Phys. J. B 12, 217 (1999)
- ²² David J. Bergman and David Stroud, in Solid State Physics, H. Ehrenreich and D. Turnbull, Eds., 46, 148 (1992).
- ²³ Ping Sheng, Phys. Rev. Lett. 45, 60 (1980)
- ²⁴ R. R. Bilboul, Brit. J. Appl. Phys. (J. Phys. D), 2, 921 (1969)
- ²⁵ W. Prellier, Ph. Lecur, and B. Mercey, J. Phys. Cond. Mat. 13, R915, (2001)
- ²⁶ W. Gotze, P. W. Lee, Phys. Rev. B 6, 1226 (1972)